Acoustic damping in resonators of langasite and langatate at elevated temperatures

Ward L. Johnson, Sudook. A. Kim
National Institute of
Standards and Technology,
325 Broadway St.,
Boulder, CO 80305, USA

Satoshi Uda
Institute for Materials Research,
Tohoku University,
2-1-1 Katahira, Aoba-ku,
Sendai, 980-8577, JAPAN

Christine F. Rivenbark
Advanced Materials Processing
and Analysis Center (AMPAC),
University of Central Florida,
Orlando, FL 32816, USA

***Abstract*—Langasite (LGS), langatate (LGT), and similar piezoelectric crystals in the *P321* crystal class have become an increasing focus of research during the past two decades, and much of the motivation for this research has been the application of these materials in high-temperature resonant acoustic sensing. The quality factor Q of these materials directly affects the resolution of sensors, and Q decreases dramatically at elevated temperatures. We present measurements and multi-frequency least-squares analysis of Q^{-1} of LGS and LGT bulk-acoustic resonators as a function of temperature that reveal a superposition of physical effects contributing to the damping, including point-defect relaxations and intrinsic phonon-phonon loss. In LGS, these effects are superimposed on a background that increases with increasing temperature. Parameters for this background obtained from least-squares analysis are found to be consistent with an anelastic dislocation mechanism with a distribution of activation energies. The absence of a significant background of this type in LGT, over the measured temperature range, and associated differences in the crystal growth and phase diagrams of LGS and LGT provide support for the view that LGT is a more attractive choice for high-temperature sensing applications.**

I. Introduction

Langasite (LGS, $La_3Ga_5SiO_{14}$) and langatate (LGT, $La_3Ga_{5.5}Ta_{0.5}O_{14}$) are synthetic piezoelectric materials with a number of characteristics that make them attractive for use in high-temperature resonant acoustic sensing. [1], [2] Their high melting temperatures (1743 K for LGS), absence of phase transitions below the melting temperature, high piezoelectric coefficients, low stress sensitivity, and ability to be grown rapidly and economically from the melt are substantial advantages, relative to quartz and perovskite ferroelectrics, for high-temperature applications. [3]–[7] However, research into optimizing the quality factor Q of LGS and LGT and determining the associated relative limitations of these materials remains in its infancy.

Previous resonant ultrasonic and electrical measurements of LGS and LGT as a function of temperature have revealed several peaks in Q^{-1} that are superimposed on a background that increases monotonically with temperature. [2], [8]–[14] The physical sources of these anelectic effects have not been determined, with the exception that Fritze, Schulz, and coworkers [2], [12] determined that the highest-temperature peak in LGS arises from movement of charge carriers in the oscillating piezoelectric field. Comparisons of the high-temperature Q^{-1} of LGS and LGT have also been very limited. [9]

In this brief report, we summarize measurements, least-squares analysis, and physical interpretation of the dependence of Q^{-1} of LGS and LGT on temperature and frequency. A more extensive description of these results, their physical interpretation, and related analysis is presented elsewhere. [15]

II. Specimens

An LGS plano-convex Y-cut resonator with a diameter of 14 mm, convex radius of 265 mm (2 diopter), and nominal fundamental frequency of 2.0 MHz was fabricated from a crystal grown by the Czochralski method from an iridium crucible in an atmosphere of argon with 2 vol.% to 4 vol.% oxygen. The methods of fabrication are described by Smythe. [16] This LGS crystal has a light orange tint, similar to that reported in previous studies of LGS and LGT grown in partial oxygen atmospheres. [17]–[19]

An LGT resonator was fabricated with orientation, diameter, convex radius, and fundamental frequency nominally identical to that of the above LGS resonator. This crystal is colorless and was grown by the Czochralski method in an atmosphere of pure nitrogen.

Following ultrasonic measurements, described below, the resonators were etched in orthophosphoric acid. Resulting dislocation pits on the surface of the LGT resonator were determined to have a density of $\sim 3 \times 10^3/\text{cm}^2$, and those on the LGS were determined to have a density one to two orders magnitude greater than this value.

III. Experimental Technique

As depicted in Fig. 1, the resonant crystal was supported near its edge on three sapphire spheres and was constrained horizontally by three larger alumina spheres. Two cylindrical copper electrodes were supported by boron nitride (BN) fixtures on opposite sides of the crystal to facilitate noncontacting piezoelectric excitation and detection of resonant vibrations. This structure was contained within a small copper chamber,

Current address of Christine Rivenbark: Krystal Engineering LLC, 1429 Chaffee Dr., Titusville, FL 32780 USA

and this small chamber was contained within a larger chamber with heaters and water-cooling tubes inside a turbo-pumped bell jar. Measurements were performed either under high vacuum or in oxygen-gettered helium with pressures in the range of 0.6 Pa to 2.7 Pa. Cooling of LGS below ambient temperatures was accomplished by passing liquid nitrogen through the tubes on the heating chamber.

Resonant modes were excited with a gated tone burst of several-millisecond duration applied to the electrodes. Q^{-1} at each temperature was determined from the rate of decay of resonant oscillations (detected with the same electrodes) following excitation, through the use of a lock-in signal-processing method. [20]

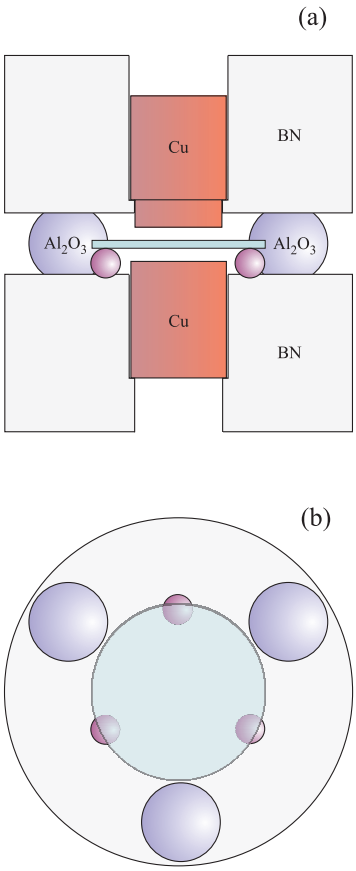

Fig. 1. Support structure and electrodes for noncontacting transduction. (a) Vertical section showing BN support structure, noncontacting Cu electrodes, and resonant crystal (light blue); supporting sapphire spheres and aligning alumina spheres closest to the vertical section are also shown. (b) View from above, with the top BN structure and Cu electrode removed, showing positions of the supporting and aligning spheres. All dimensions are to scale, with the crystal being 14 mm in diameter.

IV. Measurements and Analysis

Fig. 2 shows measurements of LGS Q^{-1} versus the inverse of temperature T from 100 K to 740 K for the three lowest thickness-shear resonant frequencies (2.03 MHz, 6.05 MHz, 9.96 MHz at the lowest measured temperature). [9] For the sake of clarity, additional measurements at 13.94 MHz are not included in this figure.

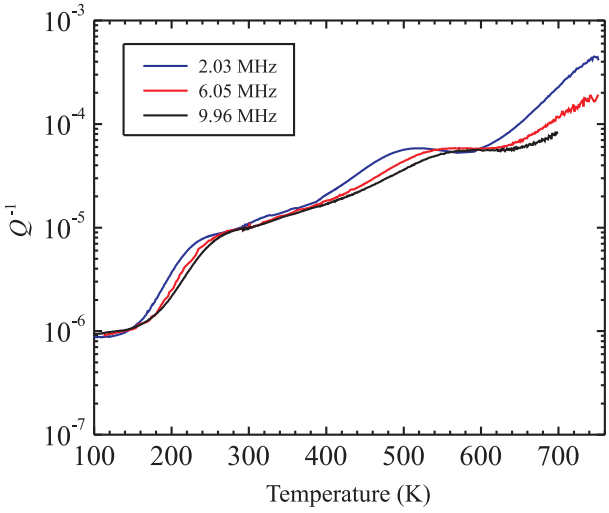

Fig. 2. Q^{-1} of LGS at 2.03 MHz, 6.05 MHz, and 9.96 MHz.

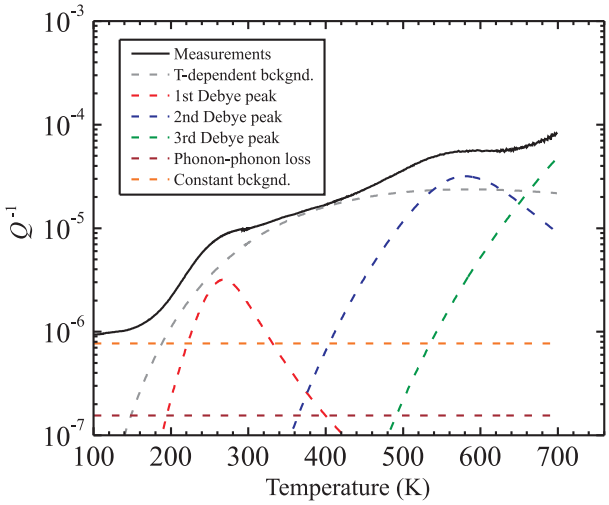

Fig. 3. Measured 10 MHz Q^{-1} of LGS and separate physical contributions at 10 MHz determined from simultaneous multifrequency least-squares fitting of function Q_f^{-1} to the data at all four measured frequencies.

Initial analysis of the LGS data [15] was pursued under the assumptions that 1) the two peaks near 260 K and 550 K (at 10 MHz) have a Debye dependence on temperature and frequency that is characteristic of anelastic point defects, [21] 2) the strongly-frequency-dependent component of the rise in Q^{-1} above ∼600 K is the shoulder of the intrinsic piezoelectric/carrier peak, [22] 3) the intrinsic phonon-phonon loss [23] is well approximated as being independent of temperature T and proportional to angular frequency ω over the measured ranges, 4) there is a broad background contribution to Q^{-1} that can be empirically expressed as increasing exponentially with T^{-1} and being proportional to ω^n, and 5) any unidentified contributions to Q^{-1} can be reasonably well approximated by a constant. Least-squares fitting of the resultant function to the LGS data, performed simultaneously at all four frequencies,

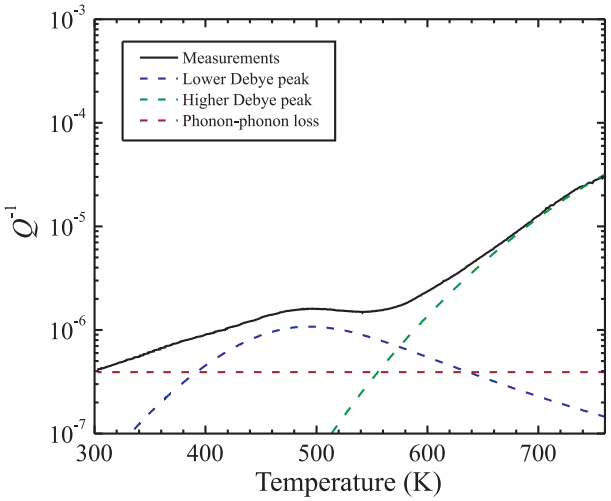

Fig. 4. Measured 10 MHz Q^{-1} of LGT and separate physical contributions at 10 MHz determined from simultaneous multifrequency least-squares fitting of function Q_f^{-1} to the data at all three measured frequencies.

provides an excellent fit. [15] However, there are two major problems with this fit. First, the relaxation strength and preexponential factor of the assumed piezoelectric/carrier relaxation are found to be inconsistent with theory and prior electrical measurements. Second, the low value of -0.15 obtained for the parameter n cannot be explained in terms of a single relaxation process.

To resolve these problems with the initial analysis, the second and third terms in the fitting function, described above, were modified. First, Q^{-1} at the highest measured temperatures was assumed to be dominated by a third point-defect relaxation, rather than the piezoelectric/carrier relaxation (which is assumed to become dominant at temperatures above the measured range). Second, the T-dependent background was assumed to arise from a distributed relaxation process, taken, for simplicity, to have a log-normal distribution of activation energies. With these modifications, Q^{-1} is assumed to have the form

$$\begin{aligned} Q_f^{-1} &= \sum_{i=1}^{3} \frac{\Delta_i}{T} \frac{\omega\tau_i}{1+\omega^2\tau_i^2} + B\omega + C \\ &\quad + \Delta_b \int_0^\infty \frac{1}{u|\ln W|(2\pi)^{1/2}} \\ &\quad \times \exp\left[\frac{-(\ln u - \ln U_b)^2}{2(\ln W)^2}\right] \frac{\omega\tau_b}{1+\omega^2\tau_b^2} du, \quad (1) \end{aligned}$$

where

$$\tau_i = \gamma_i \exp(U_i/kT), \quad (2)$$

$$\tau_b = \gamma_b \exp(u/kT), \quad (3)$$

and Δ_i, U_i, γ_i, Δ_b, U_b, γ_i, W, B, and C are fitting parameters. The summation in Q_f^{-1} includes three point-defect Debye functions. $B\omega$ represents the phonon-phonon loss and the integral represents the distributed relaxation.

Least-squares fitting of function Q_f^{-1} to the measured Q^{-1}, on a log scale, provides a close match to the LGS data over the entire range of measured temperatures and frequencies, with a standard deviation of 0.019 in $\log_{10} Q^{-1}$. The contributions from each of the terms in the fitting function Q_f^{-1} at 10 MHz are shown in Fig. 3. Between ~190 K and ~540 K, the distributed relaxation is the dominant contribution to Q^{-1}, and, at higher temperatures, the two second and third Debye peaks dominate.

The range of obtained fit parameters for U_i (0.24 eV to 0.87 eV) and γ_i (1.8×10^{-13} to 5.4×10^{-13}) are consistent with the Debye peaks arising from point-defect relaxations. Physical interpretation of the distributed relaxation is much more challenging, and this is discussed in detail elsewhere. [15] The magnitude of the mean activation energy and preexponential factor of this relaxation is found to be consistent with kink migration along dislocations in response to ultrasonic stress. The distribution of activation energies is qualitatively consistent with the fact that dislocations and associated kinks have a variety of orientations and associated energy barriers for movement.

Initial fitting of function Q_f^{-1} to LGT data acquired from 300 K to 760 K at 6.02 MHz, 10.03 MHz, and 14.03 MHz provided no evidence for a constant term C, a peak below ambient temperature, or a distributed relaxation of the form given by Q_f^{-1}. Therefore, further least-squares analysis of the LGT data was performed with these terms omitted from the fitting function. Figure 4 shows the data at 10 MHz and the results of this subsequent analysis. In this specimen, the intrinsic phonon-phonon loss is found to be dominant below ~390 K, the higher-temperature Debye peak is dominant above ~575 K, and the lower-temperature Debye peak is dominant at intermediate temperatures. Both peaks have lower relaxation strengths than their counterparts that appear at similar temperatures in LGS.

Therefore, all defect-related contributions to Q^{-1} are found to be less in the LGT specimen than in the LGS specimen studied here. The absence of a significant distributed relaxation in LGT is consistent with the much lower measured dislocation density of this specimen, relative to that of the LGS specimen. Considering the differences in crystal growth conditions of our LGS and LGT (including partial oxygen atmosphere), these results not provide a basis for direct comparison of the limits of Q in these two materials, but they are consistent with previous work indicating that defect-related loss may be more problematic in LGS. [24] In a study of a number of LGS and LGT resonators with similar crystal growth conditions, Smythe *et al* [24] found generally lower Q^{-1} in LGT at ambient temperatures, although the average difference was not as great as that measured here.

Regardless of differences in crystal growth and associated effects on Q^{-1} of the specimens studied here, our analysis of the physical mechanisms of the loss provides evidence that LGT has greater potential for high-temperature applications. In particular, the hypothesis that anelastic dislocation motion is responsible for the distributed relaxation in LGS has sub-

stantial implications for the practical optimization of these materials as resonators. Differences in the phase diagrams of LGS and LGT make it much more challenging to eliminate inclusions and associated dislocations in LGS. [15] Also, the presence of various orientations of facets at the liquid/solid interface during growth can lead to dislocation generation, and, to date, greater progress has been made in eliminating this problem in LGT. [25]

V. Conclusion

The temperature and frequency dependences of Q^{-1} of LGS and LGT reveal a superposition of physical effects, including point-defect relaxations, intrinsic phonon-phonon loss, and, in LGS, a temperature-dependent background that we suggest arises from a distributed relaxation process. We find the distributed relaxation to be consistent with anelastic kink migration along dislocations, and this hypothesis is supported by the lack of evidence for a similar distributed relaxation in the LGT resonator with a lower dislocation density. Considering intrinsic challenges of producing inclusion-free LGS crystals, our hypothesis of a distributed dislocation mechanism dominating Q^{-1} of the measured LGS over a broad temperature range leads to the further suggestion that LGT will ultimately prove to be more effective in high-temperature sensing applications.

ACKNOWLEDGMENTS

We are grateful to Mitsubishi Materials Corporation for supplying and characterizing the LGS crystal. [26] We also appreciate the contribution of employees of MTronPTI, [26] including Eric Hague and Robert Smythe, in fabricating and characterizing the resonators and the contribution of Damian Lauria in developing computer programs for the experiments.

References

[1] B. V. Mill and Y. V. Pisarevsky, "Langasite-type materials: From discovery to present state," in *Proceedings of the IEEE/IEA International Frequency Control Symposium*, 2000, pp. 133–144.

[2] H. Fritze, "High-temperature bulk acoustic wave sensors," *Meas. Sci. Technol.*, vol. 22, 012002, 2011.

[3] J. A. Kosinski, R. A. Pastore, Jr., E. Bigler, M. P. da Cunha, D. C. Malocha, and J. Detaint, "A review of langasite material constants from BAW and SAW data: Toward an improved data set," in *Proceedings of the IEEE International Frequency Control Symposium and PDA Exhibition*, 2001, pp. 278–286.

[4] B. T. Sturtevant, P. M. Davulis, and M. P. da Cunha, "Pulse echo and combined resonance techniques: A full set of LGT acoustic wave constants and temperature coefficients," *IEEE Trans. Ultrason. Ferr.*, vol. 56, pp. 788–797, 2009.

[5] Y. Kim and A. Ballato, "Force-frequency effect of Y-cut langanite and Y-cut langatate," *IEEE Trans. Ultrason. Ferr.*, vol. 50, pp. 1678-1682, 2003.

[6] Y. Jing, J. Chen, X. Gong, and J. Duan, "Stress-induced frequency shifts in rotated Y-cut langasite resonators with electrodes considered," *IEEE Trans. Ultrason. Ferr.*, vol. 54, pp. 906–909, 2007.

[7] J. A. Kosinski, R. A. Pastore, J. Yang, and J. A. Turner, "Stress-induced frequency shifts in langasite thickness-mode resonators," *IEEE Trans. Ultrason. Ferr.*, vol. 56, pp. 129–135, 2009.

[8] W. L. Johnson, S. A. Kim, D. S. Lauria, and R. C. Smythe, "Acoustic damping in langatate as a function of temperature, frequency, and mechanical contact," in *Proceedings of the IEEE Ultrasonics Symposium*, 2002, pp. 961–964, 2002.

[9] W. L. Johnson, S. A. Kim, and S. Uda, "Acoustic loss in langasite and langanite," in *Proceedings of the IEEE International Frequency Control Symposium*, 2003, pp. 646–649.

[10] W. Johnson, S. Kim, and D. Lauria, "Anelastic loss in langatate," in *Proceedings of the IEEE/EIA International Frequency Control Symposium*, 2000, pp. 186–190.

[11] H. Fritze, "High temperature piezoelectric materials: Defect chemistry and electro-mechanical properties," *J. Electroceram.*, vol. 17, pp. 625–630, 2006.

[12] M. Schulz, J. Sauerwald, D. Richter, and H. Fritze, "Electromechanical properties and defect chemistry of high-temperature piezoelectric materials," *Ionics*, vol. 15, pp. 157–161, 2009.

[13] J. Schreuer, J. Rupp, C. Thybaut, and J. Stade, "Temperature dependence of elastic, piezoelectric and dielectric properties of $La_3Ga_5SiO_{14}$ and $La_3Ga_{5.5}Ta_{0.5}O_{14}$: An application of resonant ultrasound spectroscopy," in *Proceedings of the IEEE Ultrasonics Symposium*, 2002, pp. 373–376.

[14] J. Schreuer, C. Thybaut, M. Prestat, J. Stade, and E. Haussühl, "Towards an understanding of the anomalous electromechanical behaviour of langasite and related compounds at high temperatures," in *Proceedings of the IEEE Ultrasonics Symposium*, 2003, pp. 196–199.

[15] W. L. Johnson, S. A. Kim, S. Uda, and C. F. Rivenbark, "Contributions to anelasticity in langasite and langatate," *J. Appl. Phys.*, in press.

[16] R. C. Smythe, "Material and resonator properties of langasite and langatate: A progress report," in *Proceedings of the IEEE International Frequency Control Symposium*, 1998, pp. 761–765.

[17] N. Bamba, K. Kato, T. Taishi, T. Hayashi, K. Hoshikawa, and T. Fukami, "The characteristic of the $La_3Ga_5SiO_{14}$ single crystal by vertical bridgman method in Ar atmosphere," *Mater. Sci. Forum*, vol. 510-511, pp. 842–845, 2006.

[18] H. Kimura, S. Uda, O. Buzanov, X. Huang, and S. Koh, "The effect of growth atmosphere and Ir contamination on electric properties of $La_3Ga_{5.5}Ta_{0.5}O_{14}$ single crystal grown by the floating zone and Czochralski method," *J. Electroceram.*, vol. 20, pp. 73–80, 2008.

[19] I. A. Kaurova, G. M. Kuz'micheva, V. B. Rybakov, A. B. Dubovskii, and A. Cousson, "Composition, structural parameters, and color of langatate," *Inorg. Mater.*, vol. 46, pp. 988–993, 2010.

[20] W. Johnson, "Ultrasonic resonance of metallic spheres at elevated temperatures," *J. Phys. IV*, vol. 6, pp. C8-849–852, 1996.

[21] A. S. Nowick and B. S. Berry, *Anelastic Relaxation in Crystalline Solids*. Academic: New York, 1972.

[22] A. R. Hutson and D. L. White, "Elastic wave propagation in piezoelectric semiconductors," *J. Appl. Phys.*, vol. 33, pp. 40–47, 1962.

[23] A. Akhieser, *J. Phys. (U.S.S.R.)*, vol. 1, p. 277, 1939.

[24] R. C. Smythe, R. C. Helmbold, G. E. Hague, and K. A. Snow, "Langasite, langanite, and langatate bulk-wave Y-cut resonators," *IEEE Trans. Ultrason. Ferro. Freq. Contr.*, vol. 47, pp. 355–360, 2000.

[25] C. F. Klemenz, J. Luo, and D. Shah, "High-quality 2 inch $La_3Ga_{5.5}Ta_{0.5}O_{14}$ and $Ca_3TaGa_3Si_2O_{14}$ crystals for oscillators and resonators," in *Advances in Electronic Ceramic Materials, Ceramic Engineering and Science Proceedings 26*, 2005, pp. 169–176.

[26] The identifications of the LGS crystal grower and resonator fabricator are provided here solely for the purpose of acknowledging the gratis contributions of these companies. This acknowledgement does not reflect an endorsement by NIST. We also note that the LGS crystal measured here was donated to NIST in 2002 and may not be representative of LGS currently manufactured by Mitsubishi.